Pramana - J. Phys., Vol. 36, No. 2, February 1991, pp. 191–205. © Printed in India.

Fluorescence studies of CS_2 and SO_2 at 121·6, 73·6–74·4 and 58·4 nm

I A PRAJAPATI, S M AHMED and VIJAY KUMAR
Physical Research Laboratory, Navrangpura, Ahmedabad 380009, India

MS received 23 July 1990; revised 19 October 1990

Abstract. The fluorescence spectra of CS_2 and SO_2 have been studied at three incident photon wavelengths of 121·6, 73·6–74·4 and 58·4 nm and relative production cross sections for different product states have been measured. The $CS(A\,^1\Pi \rightarrow X\,^1\Sigma^+)$ system between 240 and 290 nm has been obtained when CS_2 is photoexcited at 121·6 nm whereas $CS_2^+(B\,^2\Sigma_u^+ \rightarrow X\,^2\Pi_g)$ and $CS_2^+(A\,^2\Pi_u \rightarrow X\,^2\Pi_g)$ systems have been produced between 276 and 295 and 437 and 555 nm respectively when excited by both the incident photon wavelengths of 73·6–74·4 and 58·4 nm. The fluorescence spectra of SO_2 obtained at 121·6 and 73·6–74·4 nm include the vibrational bands of $SO(A\,^3\Pi \rightarrow X\,^3\Sigma^-)$ and $SO(B\,^2\Sigma^- \rightarrow X\,^3\Sigma^-)$ systems from 240 to 268 and 268 to 442 nm respectively whereas the emission spectrum at 58·4 nm, has contributions from the two SO systems and $SO^+(A\,^2\Pi \rightarrow X\,^2\Pi)$ system. In all these emission spectra, the fluorescence bands of different systems have been analyzed and their relative production cross sections have been measured. The results obtained in the present investigations have been compared with a few recent reliable measurements reported in literature.

Keywords. Fluorescence; photon impact; molecules; photoionization; photodissociation; dissociative photoionization.

PACS No. 33·50

1. Introduction

Sulphur dioxide and carbon disulphide are important trace constituents in the troposphere and stratosphere of the earth. Extensive data on Venusian atmospheric sulphur dioxide have been obtained from recent planetary and inter-planetary probes (Conway *et al* 1979) and from earth-based observations (Barker 1979). The evidence of SO_2 on Io was made available from in-situ UV observations by Bertaux and Belton (1979) while the detection of SO_2 frost on the Io surface was reported by Smythe *et al* (1979) from ground based infra-red measurement. The presence of CS_2 in the Venusian atmosphere has been proposed by Young (1978), even though the observational evidence for a clean detection is, at present, marginal at best. In the recent past, the CS radical has been found to be abundant in the interstellar medium (Dalgarno and Black 1976; Linke and Goldsmith 1980). The radical is most likely produced by photodissociation of CS_2. The SO_2 in the atmospheres of Venus and Io and CS_2 in the interstellar medium would interact with extreme ultraviolet photons below 100 nm and would get photoionized, photodissociated or dissociatively photoionized. As a result, the photofragments of the parent molecules and ions would be populated in higher electronic states and fluorescence from higher to lower excited states would follow provided the selection rules are allowed. The total fluorescence as well as the energy analysis of such emissions helps in understanding many

phenomena in the planetary atmospheres and interstellar medium. In view of this, an experiment has been conducted to study the dispersed fluorescence of CS_2 and SO_2 at three incident photon wavelengths of 121·6, 73·6–74·4, and 58·4 nm and relative production cross sections for different product states have been measured. These cross sections have been compared with a few recent reliable measurements reported in literature.

The three incident photon wavelengths chosen in the present experiment are H I (Lyman-α), Ne I doublet and He I resonant lines. Being part of the EUV region of the solar spectrum, these lines contribute significantly in the photophysics of the terrestrial as well as other planetary atmospheres. The hydrogen Lyman-alpha line intensity in solar spectrum is extremely large as compered to intensity at other resonant lines; the ratio of intensities could be a few orders (Hinteregger 1976). Therefore, H I Lyman-alpha would have much larger contribution in the photochemistry of the planetary atmospheres. Nevertheless, the contributions of other solar resonant lines, though small, could not be ignored.

2. Experimental set-up

The experimental set-up for studying the fluorescence from molecular ions and other photofragmented species is shown in figure 1. It consists of a microwave discharge light source, fluorescence chamber, differential pumping assembly between the light source and the fluorescence chamber, a 0·2 m monochromator positioned perpendicular to the optic axis, appropriate optics to focus the fluorescence emission at the entrance slit of the monochromator, thermoelectrically cooled photomultiplier, and a fast data acquisition system. The details regarding the various subsystems as well as the performance of the whole system are given below.

The resonant emission lines He I (58·4 nm), Ne I (73·6–74·4 nm) and H I (121·6 nm) are produced by microwave discharge of helium, neon and hydrogen respectively. The flow tube in the light source is a 6 mm dia, 20 cm long quartz tube. The light source was energized by means of microwave generator (Kiva, Opthos Instruments MD model MPG-4) with an average output power of 100 W at the frequency of 2·45 GHz. The microwave power was transmitted to the Evenson cavity, through a

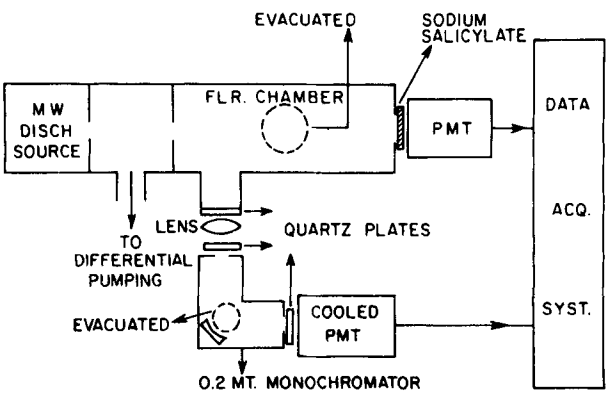

Figure 1. Schematic of the apparatus.

co-axial cable. The other end of the flow tube was connected to the differential pumping assembly and the discharge products were fast removed by a roots pump (Leybold Hearaus; pumping speed 40 lit/sec) backed by a mechanical pump (Hind Highvac, pumping speed 750 lit/min).

The other end of the differential pumping assembly was connected to the fluorescence chamber. The vacuum ultraviolet radiation was allowed to pass to the chamber through a 2 mm wide, 2·5 cm long slit. The fluorescence chamber, 6·5 cm dia and 40 cm long and made of stainless steel was evacuated to a pressure of better than 10^{-5} torr. The intensity of the resonant lines was monitored at the end of the chamber by using a combination of vacuum ultraviolet scintillator, sodium salicylate in this case and a photomultiplier of S-11 spectral response. This could be possible only when the target gas was not there in the chamber. A 0·2 meter monochromator (Minuteman Inc., USA) was positioned perpendicular to the optic axis to disperse the fluorescence emitted because of interaction of vacuum ultraviolet radiation with target molecules. The fluorescent radiation from the chamber passed through a quartz plate vacuum sealed to the chamber and a quartz lens whose focal length was chosen to match the *f*-number of the 0·2 meter monochromator. This optical system helped to focus the fluorescent radiation at the entrance slit of the monochromator. This monochromator covered the spectral range from 200 to 700 nm and had to be evacuated along with focussing assembly for studying the fluorescence in the ultraviolet region. The monochromator was vacuum sealed with two quartz plates at both the entrance and exit slit ends. The dispersed fluorescent radiation intensity was measured using a thermoelectrically-cooled photomultiplier of EMI 9558 QB type positioned behind the exit slit of the 0·2 m monochromator. In this system, total fluorescence intensity could also be measured by removing the quartz lens and monochromator system and replacing this by a thermoelectrically cooled photomultiplier. In both the cases, the photomultipliers were operated in the counting mode and after proper amplification the signals were stored in a home-made microprocessor controlled 1024 channel dual multichannel analyzer operated in the multiscaling mode. The data stored for each run was transferred to IBM compatible personal computer for data analysis.

Sulphur dioxide used in the experiment was procured from L'Air Liquide, France and was used without further purification. Carbon disulphide vapour was obtained from an analytical-grade liquid and the vapour was purified by fractional distillation before being introduced into the fluorescence chamber. The pressure in the chamber was measured absolutely using a MKS Baratron Capacitance manometer (head 310 MH-10). This was differential manometer and the pressure was made absolute by evacuating the reference side to a pressure of about 10^{-6} torr.

The resolution of the system was measured with known intense lines of mercury. It was found that the monochromator resolution at the slit width of 150 microns each for both entrance and exit slits was 0·48 and 0·8 nm at 253·7 and 404·6 nm respectively. This resolution was used for studying the CS_2^+ fluorescence spectrum of $B^2\Sigma_u^+ \rightarrow X^2\Pi_g$ system at 73·6–74·4 and 58·4 nm. For studying the fluorescence of all other systems for both SO_2 and CS_2, a monochromator resolution of 0·7 and 1·3 nm was used at 253·7 and 404·6 nm respectively which corresponded to the slit width of 400 microns each for entrance and exit slits.

3. Results and discussion

Total and dispersed fluorescence intensities were measured for both SO_2 and CS_2 at three incident photon wavelengths 58·4, 73·6–74·4 and 121·6 nm. The first two resonant emissions are energetic enough to photoionize, photodissociate and/or dissociatively photoionize both target molecules, SO_2 and CS_2 but 121·6 nm photons do not posses sufficient energy to photoionize the target gas but could photodissociate these molecules. Therefore, the total and dispersed fluorescence spectrum at this wavelength would have contribution only from the excited parent neutral molecules or photofragmented species, whereas at 58·4 and 73·6–74·4 nm, the total and dispersed fluorescence would have components from neutral and dissociated species, ionized molecules and dissociatively ionized fragments. The results obtained for both SO_2 and CS_2 would be taken up separately for detailed discussion.

3.1 *Carbon disulphide*

Total fluorescence intensities measured at various pressures of CS_2 vapour ranging from 0 to 80 m torr is shown in figure 2 at three incident photon wavelengths, 121·6, 73·6–74·4 and 58·4 nm. The fluorescence intensity measurement is relative but the pressure of the target gas has been measured absolutely. The total fluorescence intensity at the three incident photon wavelengths increases at low pressure and reaches a maximum at around 70 to 80, 15 and 20 to 25 m torr for 121·6, 73·6–74·4 and 58·4 nm photon wavelengths respectively. These maximum pressures for CS_2 have been used to study the dispersed fluorescence at these three photon wavelengths. Also, from figure 2, it is clear that the maximum fluorescence quantum yield of CS_2

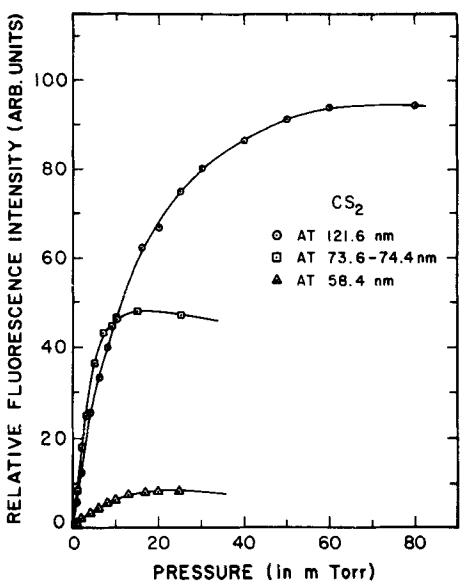

Figure 2. Total fluorescence for CS_2 as a function of pressure of the target gas at three incident photon wavelengths.

at 121·6 nm is about 1·97 and 11·1 times larger than that at 73·6–74·4 and 58·4 nm respectively.

3.1.1 *$CS(A\,^1\Pi \rightarrow X\,^1\Sigma^+)$ system*: The dispersed fluorescence for CS_2 at 121·6 nm as measured in the present experiment is shown in figure 3 in the spectral region 226 to 525 nm. Four broad peaks between 240 and 290 nm are seen in the spectrum whereas no fluorescence could be measured at other wavelengths between 226 and 240 and 290 and 525 nm. This fluorescence spectrum could not be attributed to CS_2^+ or CS^+ as it is energetically impossible to photoionize the target gas molecules at 121·6 nm. Therefore, the spectrum could only be from the parent neutral molecules or photofragmented species. The fluorescence spectrum in figure 3 has been carefully studied and has been identified to be due to $CS(A\,^1\Pi \rightarrow X\,^1\Sigma^+)$ transition. The assignment of the peaks has been made on the basis of data given by Pearse and Gaydon (1965). In the spectrum reported in the present experiment, all the vibrational bands could not be resolved. The first broad band is mainly due to (1,0) transition but has a contribution from (2, 1) and (2,0) bands also. The second broad band has main contribution from (0,0) band but other vibrational bands like (1, 1) and (2,2) also contribute significantly. The third broad band can be attributed to bands (0, 1), (1,2) and (2,3) whereas the bands (0,2), (1,3) and (2,4) form the fourth broad band. The areas under these broad bands have been measured and relative production cross sections have been calculated. The production cross section for the most intense band, in this case the second broad band, is chosen to be 1·00 and the relative cross sections

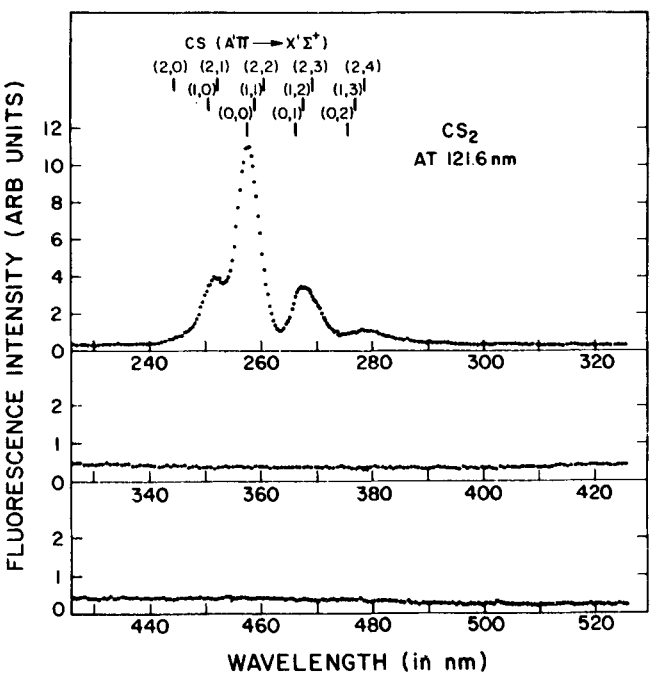

Figure 3. The fluorescence spectrum of $CS(A\,^1\Pi \rightarrow X\,^1\Sigma^+)$ system observed when CS_2 is photoexcited at an incident photon wavelength of 121·6 nm.

for other bands are obtained accordingly. At the incident photon wavelength of 121·6 nm, the relative production cross section for CS($A^1\Pi \rightarrow X^1\Sigma^+$) system in the four broad emission bands as obtained in the present experiment, have been found to be 0·36, 1·00, 0·36 and 0·11 respectively. A comparison of cross sections at other incident photon wavelengths (73·6–74·4 and 58·4 nm) is not possible as no bands corresponding to the above CS systems were observed in the dispersed fluorescence spectra at these wavelengths.

3.1.2 *$CS_2^+(B^2\Sigma_u^+ \rightarrow X^2\Pi_g)$ system*: The $B^2\Sigma_u^+ \rightarrow X^2\Pi_g$ fluorescence spectra produced by irradiation of photons at wavelengths 73·6–74·4 and 58·4 nm are shown in figures 4(a) and (b). The fluorescence emissions cover the spectral range from 276 to 295 nm. The bands shown in figures 4(a) and (b) have been assigned as per nomenclature used by Callomon (1958). The corresponding transition for each band has been given in table 1. As has been mentioned previously, the fluorescence spectra have been obtained at the monochromator resolution of 0·48 and 0·8 nm at 253·7 and 404·6 nm respectively. Even though this resolution is sufficiently large for this type of experiment, some of the bands, have not been resolved. Band α does not appear in the fluorescence spectrum obtained at the incident photon wavelength 73·6–74·4 but it appears in the spectrum at incident wavelength 58·4 nm even though it is partially resolved. The band *w*, which in fact is a combination of three bands assigned as *v*, *w* and *x* is not resolved in the two spectra. The bands *f* and *y* are nicely resolved in figure 4(b) whereas they appear as a single broad band in figure 4(a). A few new bands below 279 nm and above

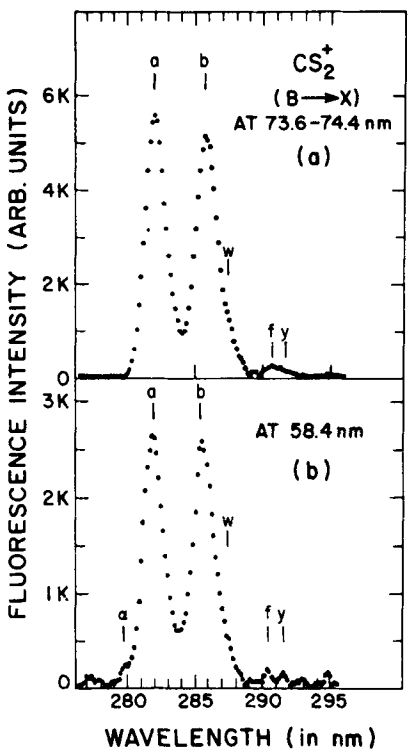

Figure 4. The fluorescence spectra of $CS_2^+(B^2\Sigma_u^+ \rightarrow X^2\Pi_g)$ system when excited at an incident photon wavelengths of (**a**) 73·6–74·4 nm and (**b**) 58·4 nm.

Table 1. The band head positions and assignment as given by Callomon (1958) and the relative production cross sections for various bands of $CS_2^+(B^2\Sigma_u^+ \rightarrow X^2\Pi_g)$ system produced by photons at a few incident wavelengths.

Band Head			Relative production cross sections		
			Present work at incident wavelength		Lee *et al* (1975) at incident wavelength
λ in nm	Assignment	Transition $B^2\Sigma_u^+ \rightarrow X^2\Pi_g(\Omega)$	73·6–74·4 nm	58·4 nm	55·5–82·7 nm
279·80	α	(020)→(020)(3/2)	—	0·09	—
282·00	a	(000)→(000)(3/2)	1·00	1·00	1·00
285·55	b	(000)→(000)(1/2)	0·92	0·98	0·86
287·35	v		not resolved	not resolved	0·06
287·40	w				
287·65	x				
290·80	f	(000)→(100)(1/2)	0·04	0·12	0·02
291·35	y		0·03	0·12	0·02

292 nm could be seen in figure 4(a). No attempt has been made to identify these bands. The relative production cross section for all these bands of the $CS_2^+(B^2\Sigma_u^+ \rightarrow X^2\Pi_g)$ system produced by photons at incident wavelengths of 73·6–74·4 and 58·4 nm have been obtained and are given in table 1. Also given in the table are the relative production cross sections of all these bands reported by Lee *et al* (1975) at incident wavelengths 55·5–82·7 nm. It is clear that the relative production cross sections reported in the present experiment for the bands b, f and y much larger at incident wavelength of 58·4 nm as compared to those at 73·6–74·4 nm. The average values of relative production cross sections for these bands reported by Lee *et al* (1975) at indident photon wavelengths ranging from 55·5 to 82·7 nm are in general, smaller than values reported in the present work.

3.1.3 $CS_2^+(A^2\Pi_u \rightarrow X^2\Pi_g)$: The fluorescence spectrum in the wavelength region 437–555 nm produced by the interaction of vacuum ultraviolet photons of wavelengths 73·6–74·4 and 58·4 nm with CS_2 vapour is shown in figures 5(a), (b) and (c). The present spectrum has been identified as the $CS_2^+(A^2\Pi_u \rightarrow X^2\Pi_g)$ system by Weissler *et al* (1971). The assignment of the different vibrational bands as obtained in the present experiment have been made using the wavelength data given by Weissler *et al*.

It is known that the states $A^2\Pi_u$ and $X^2\Pi_g$ are both doubly degenerate having spin-orbit splitting corresponding to $\Omega = 1/2$ and 3/2. From the analysis of the $CS_2^+(B^2\Sigma_u^+ \rightarrow X^2\Pi_g)$ system, Callomon (1958) has determined that the vibrational levels of $X^2\Pi_{g,1/2}(000)$ and $X^2\Pi_{g,3/2}(000)$ are inverted, with a splitting of 440·71 cm^{-1}. On the other hand, the splitting in the vibrational levels of $CS_2^+(A^2\Pi_u)$ state is not yet known. In the present fluorescence spectrum (figure 5), no vibrational transition corresponding to spin-orbit split components of $A^2\Pi_u$ state of CS_2^+ could be observed. It appears that the spin-orbit splitting for this state is quite small. A similar inference has been drawn by Lee *et al* (1975) from their fluorescence measurements and Brundle and Turner (1969) from their photoelectron spectroscopic studies of the molecular ion.

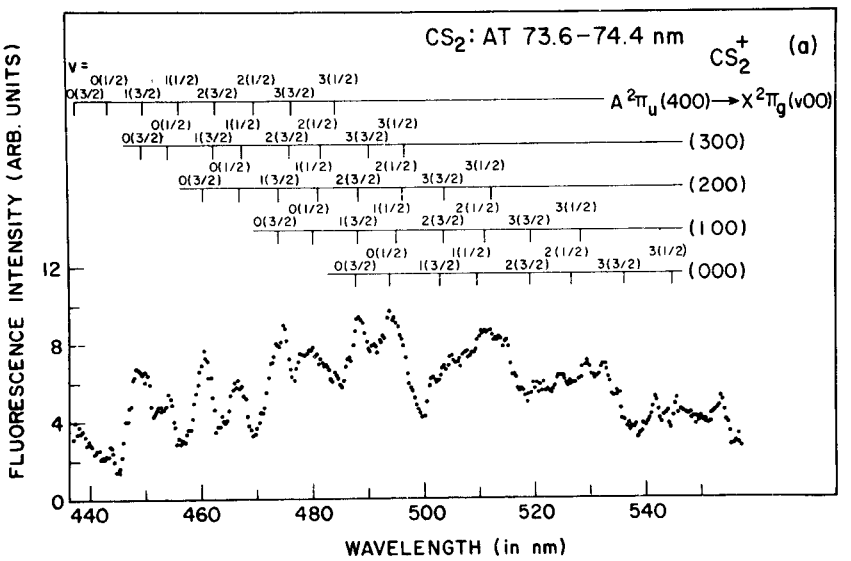

Figure 5(a). The fluorescence spectra of $CS_2^+ (A\,^2\Pi_u \rightarrow X\,^2\Pi_g)$ system when excited at an incident photon wavelength of 73·6–74·4 nm.

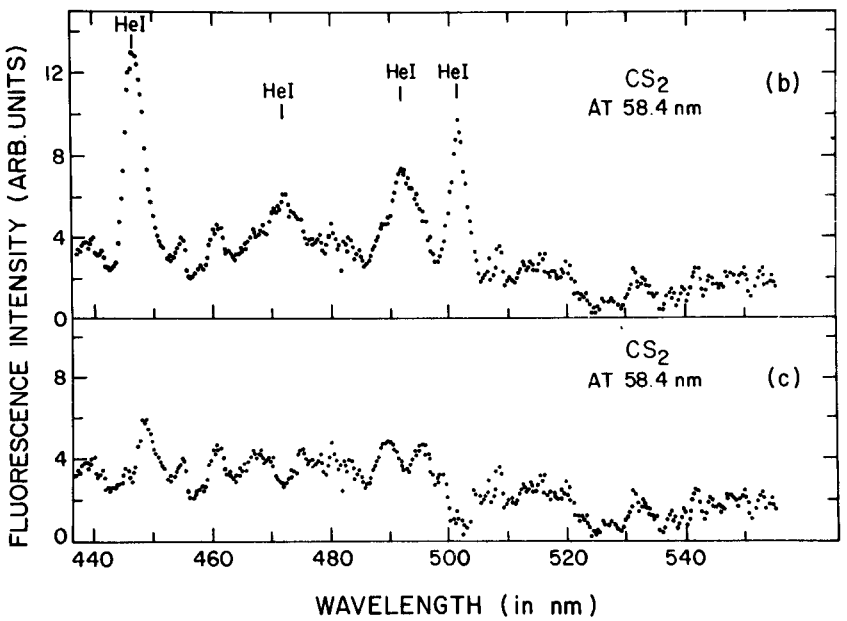

Figures 5(b) and (c). The fluorescence spectra of $CS_2^+ (A\,^2\Pi_u \rightarrow X\,^2\Pi_g)$ system when excited at an incident photon wavelength of 58·4 nm. **(b)** shows the fluorescence spectrum along with the scattered radiation from incident helium line. In **(c)**, the scattered radiation from helium line has been subtracted from the fluorescence spectrum.

The fluorescence spectra of CS_2 at helium and neon resonant lines in the vacuum ultraviolet region shows the occurrence of the helium lines in the visible region scattered from the fluorescence chamber as well as from the target gas. This is possible as the energy selection of the incident photons has not been carried out using any

type of dispersing element. This has helped in preventing any loss of intensity of 73·6–74·4 and 58·4 nm lines. But it has allowed the other emission lines of neutral helium to get scattered in the fluorescence chamber and enter the monochromator used for dispersing the fluorescence emissions. This effect is predominant in the case of helium lines in the ultraviolet and visible regions but is negligibly small in the case of neon lines. These scattered helium lines have been reproduced in another experiment under similar experimental conditions but without the target gas. This scattered line spectrum has been subtracted from the fluorescence spectrum at 58·4 nm. The fluorescence spectrum without subtraction of scattered radiation has been shown in figure 5(b) whereas the spectrum after proper subtraction of scattered radiation is shown in figure 5(c).

The relative production cross sections for the various emission wavelengths produced by incident photon wavelengths (73·6–74·4 and 58·4 nm) are given in table 2 for the $CS_2^+ (A\,^2\Pi_u \rightarrow X\,^2\Pi_g)$ system. Each emission wavelength region includes more than one vibrational bands. The transition for these bands are also given in the table. The relative production cross sections obtained in the present experiment at two incident photon wavelengths are compared with the data reported by Lee *et al* (1975) obtained at an incident photon wavelength of 92·3 nm. The emission wavelength regions in the two experiments are not exactly the same as the resolution in the two experiments are different. The measurements reported by Lee *et al* have been carried out at better resolution; therefore the emission wavelength regions in their case are extended on both sides. Also the relative production cross sections for the fifth emission wavelength region has been fixed at 1·00 and cross sections for other regions have been calculated accordingly. This has been done in spite of the fact that the area under this region is not the maximum. This is because for the similar wavelength region, the relative production cross section has been fixed at 1·00 by Lee *et al* (1975); therefore the comparison becomes simpler.

A direct comparison of the relative production cross sections measured in the present work with those reported by Lee *et al* (1975) is not exactly possible as both these measurements have been carried out at different incident photon wavelengths. It is clear from table 2 that for a given emission wavelength region, the relative cross sections are different at three incident photon wavelengths. In the last few emission wavelength regions, the relative production cross sections appear to increase as the incident photon wavelength increases. It has been shown by Dibeler and Walker (1967) in their ion mass spectrometric studies that at wavelengths shorter than 80 nm, the dissociative ionization processes $CS_2 + h\nu \rightarrow S^+ + CS + e$ and $CS^+ + S + e$ have appreciable efficiencies. Since these dissociative ionization processes will reduce the production of CS_2^+ ions, the cross sections for the production of fluorescence from excited CS_2^+ ions may be expected to decrease at shorter incident photon wavelength.

3.2 *Sulphur dioxide*

Total fluorescence intensity measured at various pressures of sulphur dioxide gas from 0 to 60 mtorr is shown in figure 6, at three incident photon wavelengths, 121·6, 73·6–74·4, and 58·4 nm. The total fluorescence intensity at the three incident wavelengths increases at low pressures and reaches a maximum at around 30 mtorr for all the three wavelengths. This maximum pressures for SO_2 has been used to study the dispersed fluorescence at different incident wavelengths. Also, from figure 6, it is clear

Table 2. The relative production cross sections for $CS_2^+(A\,^2\Pi_u \rightarrow X\,^2\Pi_g)$ system in various emission wavelength regions. Also given are the transitions in different wavelength regions.

Emission wavelength region in nm	Transition $CS_2^+: A\,^2\Pi_u \rightarrow X\,^2\Pi_g(\Omega)$	Relative production cross sections		
		Present work		Lee *et al* (1975)
		at 58·4 nm	at 73·6–74·4 nm	at 92·3 nm
445·0–451·3	(300)→(000)(3/2) (400)→(100)(3/2)	1·29	0·63	0·43
451·3–456·3	(300)→(000)(1/2)	0·74	0·48	0·43
456·3–463·0	(200)→(000)(3/2) (300)→(100)(3/2)	1·08	0·75	0·63
463·0–470·0	(200)→(000)(1/2) (300)→(100)(1/2)	1·12	0·68	0·75
470·0–476·7	(100)→(000)(3/2) (200)→(100)(3/2)	1·00	1·00	1·00
476·7–485·5	(100)→(000)(1/2) (200)→(100)(1/2) (300)→(200)(1/2)	1·42	1·33	0·93
485·5–492·0	(000)→(000)(3/2) (100)→(100)(3/2) (200)→(200)(3/2) (300)→(300)(3/2)	1·11	1·18	1·07
492·0–500·0	(000)→(000)(1/2) (100)→(100)(1/2) (200)→(200)(1/2) (300)→(300)(1/2)	1·23	1·35	1·41
500·0–519·0	(000)→(100)(3/2) (100)→(200)(3/2) (200)→(300)(3/2) (000)→(100)(1/2) (100)→(200)(1/2) (200)→(300)(1/2)	1·73	2·92	2·46
519·0–538·0	(000)→(200)(3/2) (100)→(300)(3/2) (000)→(200)(1/2) (100)→(300)(1/2) (000)→(300)(3/2)	1·04	2·47	3·02
538·0–555·0	(000)→(300)(1/2) and others	1·35	1·60	2·32

that the maximum fluorescence quantum yeild of SO_2 at 121·6 nm is about 6·8 and 7·3 times larger than that obtained at 73·6–74·4 and 58·4 nm respectively.

The fluorescence spectra for SO_2 excited at three incident photon wavelengths 121·6, 73·6–74·4 and 58·4 nm were obtained in the emission wavelength region from 238 to 442 nm. The monochromator resolution of 0·7 and 1·3 nm at 253·7 and 404·6 nm respectively was adequate to identify most of the measured band heads in all the fluorescence spectra shown in figure 7. The fluorescence spectrum at the incident

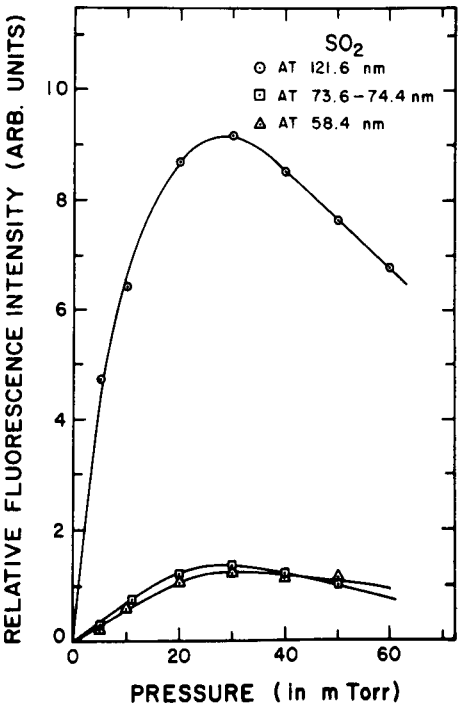

Figure 6. Total fluorescence for SO_2 as a function of pressure of the target gas at three incident photon wavelengths.

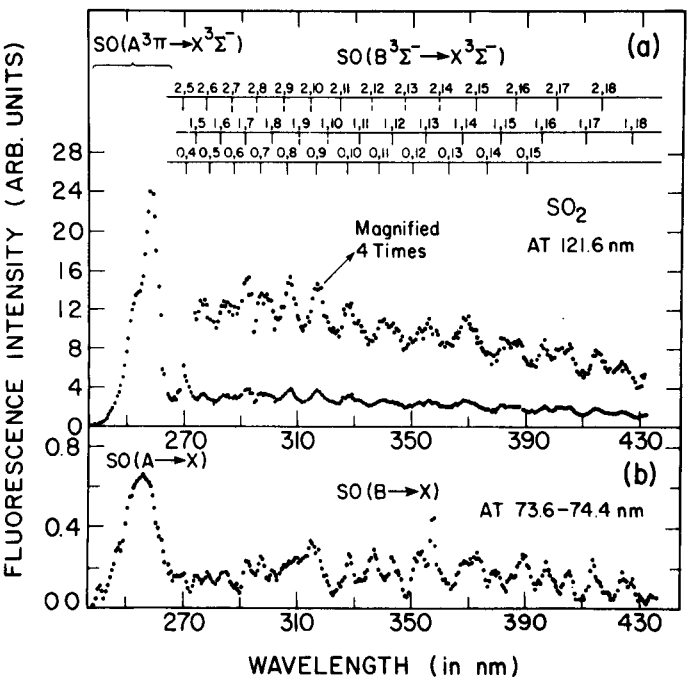

Figure 7(a) and (b). The fluorescence spectra of SO_2 at incident photon wavelengths of 121·6 nm and 73·6–74·4 nm.

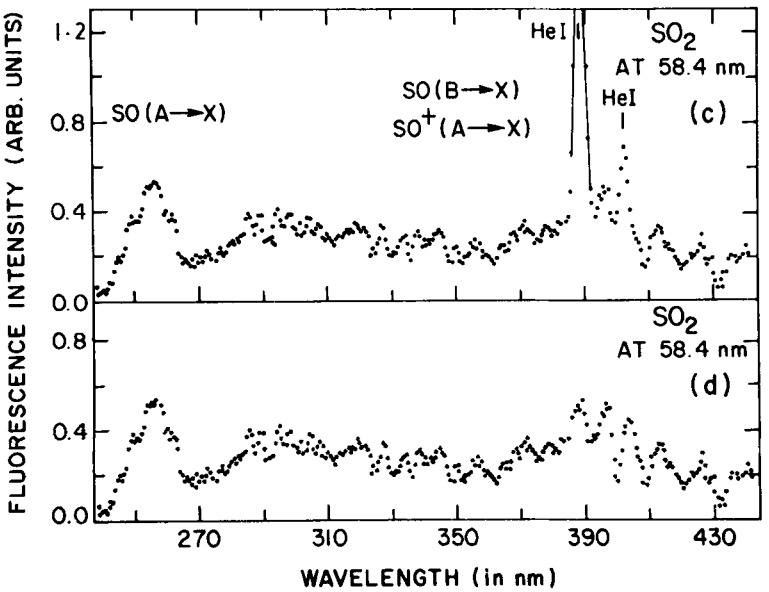

Figure 7(c) and (d). The fluorescence spectra of SO_2 at incident photon wavelength of 58·4 nm. (c) shows the fluorescence spectrum along with scattered radiation of helium line whereas (d) shows the fluorescence spectrum after proper subtraction of scattered radiation.

photon wavelength of 121·6 nm (figure 7a) includes vibrational bands of two systems of SO emission. The $A\,^3\Pi \rightarrow X\,^3\Sigma^-$ system of SO extends from 240 to 268 nm whereas the $B\,^3\Sigma^- \rightarrow X\,^3\Sigma^-$ system covers the spectral range from 268 to 442 nm. The emission spectrum in the two regions has been identified and the assignment of bands has been carried out using the wavelength data reported by Rosen (1970). It may be noted that the dotted lines shown in the assignment chart in figure 7(a) have not been observed and reported by Rosen (1970), but these have been shown in the figure based on simple calculations using molecular constants reported in literature.

The fluorescence spectrum at incident photon wavelength of 73·6–74·4 nm (figure 7b) includes the bands of the same two systems of SO as observed in case of excitation at 121·6 nm but the emission spectrum is very much weaker. The fluorescence spectrum from SO_2^+ though energetically possible (table 3) has not been observed. It is possible that the SO_2^+ fluorescence is very weak and could not be identified because of the presence of the stronger emission from SO. Dujardin and Leach (1981) have shown previously in their photoion-fluorescence photon coincidence study that the emission from SO fragments is about 100 times stronger than the SO_2^+ emission when excited at the Ne I incident photon wavelength.

The emission spectrum as shown in figures 7(c) and (d) was obtained by photoionization of SO_2 at the incident photon wavelength of 58·4 nm. Some of the scattered neutral helium line emissions observed in the present work could be seen in figure 7(c). These lines have been subtracted from the fluorescence spectra in the same way as in the case of CS_2. The fluorescence spectra without subtraction of scattered radiation has been shown in figure 7(c) whereas the spectra after proper subtraction of scattered radiation is shown in figure 7(d). This spectrum differs

Table 3. Threshold energies for formation of various electronic excited states of products for the photoexcitation process of SO_2.

Products	Threshold energies (eV)	Fluorescence wavelength observed in the present work (in nm)
$SO_2^+(\tilde{X}^2A_1)+e^-$	12·30	
$SO_2^+(\tilde{A}^2A_2)+e^-$	13·01	
$SO_2^+(\tilde{B}^2B_2)+e^-$	13·24	
$SO_2^+(\tilde{C}^2B_2)+e^-$	15·99	
$SO_2^+(\tilde{D}^2A_1)+e^-$	16·32	
$SO_2^+(\tilde{E}^2B_1)+e^-$	16·50	
$SO_2^+(\tilde{F}^2A_1)+e^-$	20·06	
$SO^+(X^2\Pi)+O(^3P)+e^-$	15·93	
$SO^+(a^4\Pi)+O(^3P)+e^-$	19·12	
$SO^+(A^2\Pi)+O(^3P)+e^-$	20·32	$SO^+(A\rightarrow X)$: $\geqslant 250$
$SO^+(b^4\Sigma^-)+O(^3P)+e^-$	20·56	
$SO(X^3\Sigma^-)+O(^3P)$	5·65	
$SO(A^3\Pi)+O(^3P)$	10·40	$SO(A\rightarrow X)$: $\geqslant 240$
$SO(B^3\Sigma^-)+O(^3P)$	10·81	$SO(B\rightarrow X)$: $\geqslant 258$

significantly from the spectra shown in figures 7(a) and (b). It consists of two components given below:

a) The first component of the emission spectrum is the same as for spectra excited at other two incident photon wavelengths i.e. the $A^3\Pi\rightarrow X^3\Sigma^-$ system of SO. This system is slightly weaker than that observed in figure 7(b). But it is much stronger than that observed by Dujardin and Leach (1981) at the same excitation wavelength, 58·4 nm. Surprisingly, this system was not observed by Wu (1984) in the emission spectra obtained at the two excitation wavelengths, 68·6 and 55·5 nm.

b) The second component of the emission spectrum includes a broad continuum band with discrete bands of SO and SO^+ superimposed on it. The broad continuum band extends over the range from 260 to 440 nm with two apparent maxima at around 300 and 390 nm. One of the sets of bands superimposed over the continuum belongs to $SO(B^3\Sigma^-\rightarrow X^3\Sigma^-)$ system which extends almost over the whole spectral range from 268 to 442 nm. This system is relatively very weak. There is another set of bands superimposed over the continuum which is very weak from 250 to 380 nm but a few clearly resolved discrete bands were observed in the spectral region 380 to 440 nm. This set of bands belong to $SO^+(A^2\Pi\rightarrow X^2\Pi)$ system. The assignment for the bands of the system has recently been carried out by Tsuji *et al* (1980). The bands of the two systems mentioned above are very close to each other; therefore some of the bands of the two systems appear to be a single broad band. Also, because of this type of merging and poor resolution, these bands appear to be superimposed over a continuum. It should be added that no emission due to SO_2^+ excitation was observed as shown in figures 7(c) and (d). Threshold energies for formation of some electronic excited states of the products are given in table 3 for the photoexcitation process of SO_2.

The relative production cross sections for $SO(A^3\Pi\rightarrow X^3\Sigma^-)$ and $SO(B^3\Sigma^-\rightarrow X^3\Sigma^-)$ systems have been calculated at the incident photon wavelengths of 121·6, and

Table 4. The relative production cross sections for $SO(A^3\Pi \rightarrow X^3\Sigma^-)$ and $SO(B^3\Sigma^- \rightarrow X^3\Sigma^-)$ systems produced at incident photon wavelengths of 121·6 and 73·6–74·4 nm.

Incident photon wavelength in nm	Relative production cross sections	
	$SO:A \rightarrow X$ system	$SO:B \rightarrow X$ system
121·6	0·57	1·00
73·6–74·4	0·35	1·00

73·6–74·4 nm. These cross sections include all the vibrational transitions for the two SO systems. No attempt has been made to calculate the relative cross sections for individual bands. For this purpose, the production cross section for the $B \rightarrow X$ system has been considered to be 1·00 and that for the $A \rightarrow X$ system has been calculated accordingly. It may be mentioned here that the relative production cross sections at the incident photon wavelength of 58·4 nm have not been computed as at this wavelength, there are large number of interspaced bands belonging to a few systems mentioned above. The relative production cross sections at 121·6 and 73·6–74·4 nm are given in table 4. The ratio of $A \rightarrow X$ system to $B \rightarrow X$ system has been found to be 0·57 and 0·35 at the excitation wavelengths of 121·6 and 73·6–74·4 nm. No comparison with any other data has been carried out as the production cross sections for these systems have not been reported in literature.

4. Conclusion

The fluorescence spectra of CS_2 and SO_2 have been studied at three incident photon wavelengths of 121·6, 73·6–74·4 and 58·4 nm and relative production cross sections for different product states have been measured. The fluorescence spectra and relative production cross sections thus obtained have been compared with a few recent reliable measurements wherever possible. The $CS(A \rightarrow X)$ system produced at 121·6 nm and CS_2^+ ($B \rightarrow X$ and $A \rightarrow X$) systems obtained at 73·6–74·4 and 58·4 nm have been analyzed in the present work whereas the $SO(A \rightarrow X$ and $B \rightarrow X)$ systems at 121·6 and 73·6–74·4 nm and the two systems of SO along with $SO^+(A \rightarrow X)$ system at incident photon wavelength of 58·4 nm have been studied carefully. In all these emission spectra, the relative production cross sections for fluorescence bands of different systems have been computed. It may be noted that not much work has done in this direction. Therefore, a comprehensive comparison is not at all possible.

In all these measurements carried out in the present work, the monochromator resolution was not enough to resolve all the bands individually. Instead, the relative production cross sections for different spectral regions consisting of large number of vibrational bands, were computed. It is felt that more measurements in this direction are required with much higher monochromator resolution without sacrificing the low level fluorescence intensities.

Also, in the present experiment as well as in other studies reported by a few other researchers, the relative production cross sections have been measured at a few incident photon wavelengths only. This does not give a complete picture about the possible change of cross section as a function of incident photon energy. To get a better insight, the measurements are required to be carried out at a large number of incident photon wavelengths.

References

Barker E S 1979 *Geophys. Res. Lett.* **6** 117
Bertaux J L and Belton M J S 1979 *Nature (London)* **282** 813
Brundle C R and Turner D W 1969 *Int. J. Mass Spectrom. Ion Phys.* **2** 195
Callomon J H 1958 *Proc. R. Soc. London* **A244** 220
Conway R R, McCoy R P and Barth C A 1979 *Geophys. Res. Lett.* **6** 629
Dalgarno A and Black J H 1976 *Rep. Prog. Phys.* **39** 573
Dibeler V H and Walker J A 1967 *J. Opt. Soc. Am.* **57** 1007
Dujardin G and Leach S 1981 *J. Chem. Phys.* **75** 2521
Hinteregger H E 1976 *J. Atmos. Terr. Phys.* **38** 791
Lee L C, Judge D L and Ogawa M 1975 *Can. J. Phys.* **53** 1861
Linke R A and Goldsmith P F 1980 *Astrophys. J.* **235** 437
Pearse R W B and Gaydon A G 1965 *The identification of molecular spectra*, (London: Chapman and Hall)
Rosen B 1970 *Spectroscopic data relative to diatomic molecules* (Oxford: Pergamon) p. 342
Smythe W C, Nelson R M and Nash D B 1979 *Nature (London)* **280** 766
Tsuji M, Yamagiwa C, Endoh M and Nishimura Y 1980 *Chem. Phys. Lett.* **73** 407
Weissler G L, Ogawa M and Judge D L 1971 *J. Phys. Paris, Suppl.* **32** C4–154
Wu C Y R 1984 *J. Phys.* **B17** 405
Young A T 1978 *Bull. Am. Astron. Soc.* **10** 549